

# Influence of precursor morphology on the microstructure of silicon carbide nanopowder produced by combustion syntheses

Zhanna Yermekova<sup>a</sup>, Zulkhair Mansurov<sup>a</sup>, Alexander Mukasyan<sup>b,\*</sup>

<sup>a</sup> *al-Farabi Kazakh National University, 71 al-Farabi Ave., Almaty 050038, Kazakhstan*

<sup>b</sup> *Department of Chemical and Biomolecular Engineering, University of Notre Dame, Notre Dame, IN 46556, USA*

Received 23 April 2010; received in revised form 28 April 2010; accepted 4 June 2010

Available online 4 August 2010

## Abstract

Silicon carbide nanopowder was synthesized using the combustion-based approach. Combustion synthesis was performed in reduction type  $\text{SiO}_2\text{--Mg--C}$  system. Silicon oxide powders with different morphologies and average particle size were used as starting powders. It was shown that even micro-size silica allows formation of nano-size silicon carbide powder. However, the specific surface area of synthesized SiC particles increases with the decrease the size of the silicon oxide precursor. The mechanism of silicon carbide formation in the combustion wave is also discussed.

© 2010 Elsevier Ltd and Techna Group S.r.l. All rights reserved.

**Keywords:** Silicon carbide; Nanopowder; Combustion synthesis; Self-propagating high-temperature synthesis

## 1. Introduction

The unique properties of silicon carbide define a variety of its applications including the nuclear power industry (radiation and temperature resistance), chemical and natural-gas industry (chemical stability), power electronics (limited capacitive losses, considerable forward currents and high inverse voltage), space technology (low material density) and auto-industry [1,2]. The method for silicon carbide production depends on the desired material structure, the form and shape of the final product and its application. Several approaches for SiC synthesis have been developed [3]. The most widely used method is based on the thermal reduction of silica by carbon, where different types of the silicon containing precursors, such as dry silica powder [4], liquid glass [5], sugar [6], gel [7], and even waste [8] were utilized. The reduction of silica by pure silicon is also known [cf. 9]. Another method for the synthesis of high purity SiC phases is chemical vapor deposition [10–12]. However in all above cases, the cost, time and energy expenses are still comparatively high. It is also a big challenge to produce nano-size silicon carbide particles in large volumes. Thus it

is important to develop novel approaches for the synthesis of fine SiC powders.

Combustion synthesis (CS) is a unique process which involves self-sustained exothermic heterogeneous reactions to produce a variety of advanced materials [13]. In a conventional CS scheme, so-called self-propagating high-temperature synthesis (SHS) mode, a reactive mixture of solid powders is ignited at one end and a high-temperature combustion wave propagates through the media, converting the precursors to a desired product. The SHS method has several advantages over traditional powder metallurgical technologies [14]. These advantages include (i) short (~minutes) synthesis time; (ii) energy saving, since the internal system chemical energy is primarily used for materials production; (iii) simple technological equipment; (iv) ability to produce high purity products, since the extremely high-temperature conditions (up to 4000 K), which takes place in the combustion wave, burns off most of the impurities. This approach also offers the possibilities for nanomaterials production [15,16].

In this work different  $\beta$ -SiC nanopowders were synthesized using SHS in  $\text{SiO}_2\text{--Mg--C}$  system. Special attention was paid on the influence of the precursor (silica) morphology on the microstructure of the final product. It was shown that under optimum synthesis conditions even micro-size silica allows formation of a silicon carbide nanopowder. However, the

\* Corresponding author. Tel.: +1 574 631 9825; fax: +1 574 631 8366.

E-mail address: [amoukasi@nd.edu](mailto:amoukasi@nd.edu) (A. Mukasyan).

specific surface area of produced SiC particles increases with the decrease of the size of silicon oxide precursor. The mechanism of silicon carbide formation in the combustion wave is also discussed.

## 2. Combustion synthesis of silicon carbide

It is well recognized that the reaction between silicon and carbon to produce silicon carbide, i.e.  $\text{Si} + \text{C} \rightarrow \text{SiC}$ , has moderate enthalpy of formation (only  $\Delta H_{273} = -17.5 \pm 0.5$  kcal/mol; compared to  $\Delta H_{273} = -55.5 \pm 0.5$  kcal/mol for Ti–C system) and thus possesses relatively low adiabatic combustion temperature ( $\sim 1800$  K compare 3290 K for Ti–C reaction). Thus in this system it is not easy to accomplish a self-sustained SHS process. However, almost all available literatures on SHS of silicon carbide are related to this chemical pathway.

The first publication on this matter by Martinenko and Borovinskaya is dated 1978 and reported the results on direct combustion synthesis of SiC from the elements by using *preliminary preheating* of the reactive media [17]. The mechanism of SiC formation in CS wave has been proposed by Narayan et al. [18]. Experiments were conducted in not well-defined conditions, i.e. initial sample temperature before

reaction initiation was not measured. But detailed analysis of experimental conditions leads to the conclusion that again preheating of initial powder mixture allowed authors to arrange the self-sustained mode of combustion wave propagation. The following steps for  $\beta$ -SiC formation in SHS wave were suggested: (i) melting of silicon; (ii) spreading of melted Si along the surface of solid carbon particles with simultaneous formation of a thin carbide layer; (iii) carbon dissolution in the melt; and (iv) solid SiC grain precipitation in the liquid solution. The general approach to increase the adiabatic combustion temperature by preliminary preheating of the reaction media, has been used by many other authors [cf. 19,20].

Other methods to enhance the reactivity of Si–C system include:

- SHS synthesis in Si–C–air/nitrogen systems, where additional solid–gas reactions contribute to the system exothermicity [21,22];
- the use of different chemical activated additives (polytetrafluoroethylene, carbamide, etc.) to change reaction pathways [23–27];
- the use of additional electrical field [28] and;

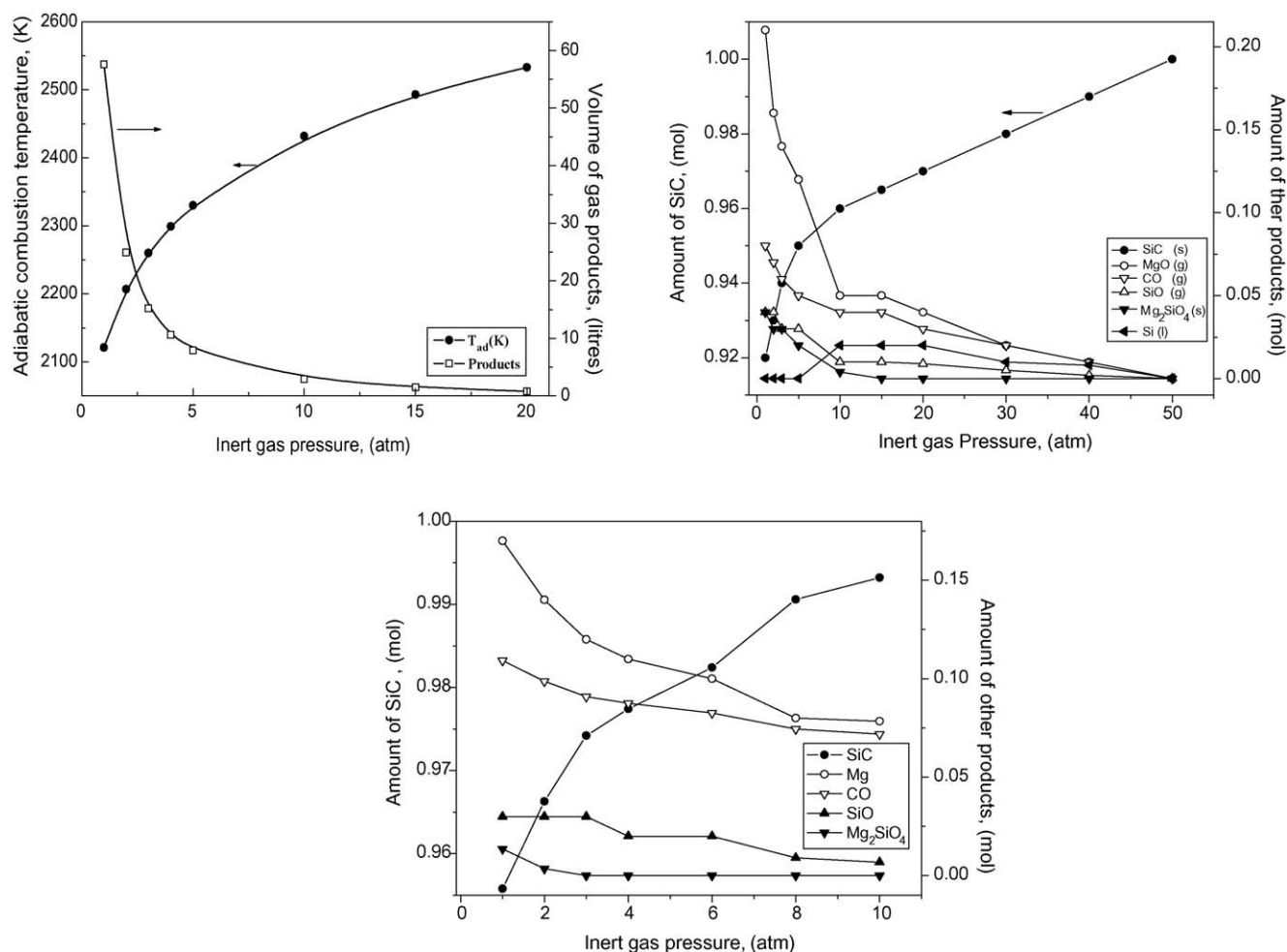


Fig. 1. Thermodynamic characteristics of the investigated system as a function of inert gas pressure for different compositions of initial  $\text{SiO}_2\text{:Mg:C}$  mixture: (a and b) 1:2:1; (c) 1:2:1.065.

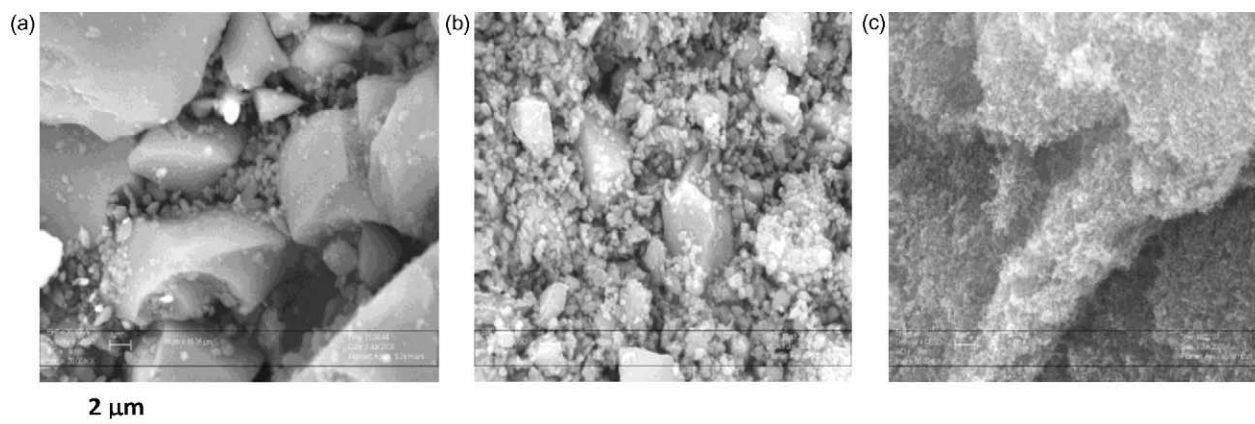


Fig. 2. Microstructure of the initial  $\text{SiO}_2$  powders: (a) KZ; (b) Cerac; (c) UFS.

(d) mechanical activation of the initial mixture [29,30].

The other way to produce SiC powder using SHS method involves sequence of two reactions that take place in the combustion front: reduction of silica by a metal to make pure silicon, followed by silicon reaction with carbon. The  $\text{SiO}_2 + \text{Me}(\text{Mg}, \text{Al}) + \text{C}$  system is much more exothermic, as compared to binary  $\text{Si} + \text{C}$  composition (see below). Thus it is relatively easy to initiate the SHS mode in such reduction-type mixture without using any special enhancing means. However, only few patents may be found that are related to the combustion synthesis of silicon carbon through the reduction of silica [31,32], while essentially no other information on this process is available in the literature. Let us discuss this approach in detail.

### 3. Thermodynamic considerations

The overall combustion reaction for reduction synthesis of SiC, when magnesium (Mg) is used as a reducing element, can be written as follows:



The thermodynamic analysis [33,34] allows calculating the adiabatic combustion temperature ( $T_{\text{ad}}$ ) and equilibrium products composition for reaction (1) as a function of the inert gas (argon) pressure ( $P$ ) in the reaction chamber (Fig. 1). It can be seen (Fig. 1a) that  $T_{\text{ad}}$  increases and the amount of gas phase products decreases, with increase of inert gas pressure. Also the absolute value of  $T_{\text{ad}}$  is  $>2000$  K, which is above melting (m.p.) and boiling (b.p.) points of magnesium (922 K and 1363 K, correspondingly), m.p. of silicon (1683 K) and silicon oxide (1923 K), but well below m.p. of magnesium oxide (3073 K) and carbon (4093 K). It is also clear that the amount of gaseous products (which includes Mg, CO and SiO) can be lowered by increasing gas pressure in the reaction chamber, because higher  $P$  suppresses the gasification processes.

In addition to main solid products, i.e. SiC and MgO, two other phases, i.e.  $\text{Mg}_2\text{SiO}_4$  and Si, can be produced (Fig. 1b). The last two phases are undesirable, because it is not easy to leach them out from the as-synthesized product. Thermodynamics suggests how one can reduce the amount of these phases. It

appears that increasing of  $P$  leads to a significant decrease of the  $\text{Mg}_2\text{SiO}_4$  and Si quantities. Moreover at  $P = 50$  atm only SiC and MgO are the equilibrium combustion products in the considered system (Fig. 1b). Thus 100% of  $\text{SiO}_2$  conversion to silicon carbide for stoichiometric 1:2:1 composition can be reached under high argon pressure. However, if it is a requirement to conduct synthesis under moderate gas pressure ( $P \leq 10$  atm) the other approach can be used for full conversion of  $\text{SiO}_2$  to silicon carbide. Fig. 1c shows the equilibrium products for slightly not stoichiometric mixture with small excess of carbon (1:2:1.065). It can be seen that for this composition 0.995 mole of SiC can be produced at relatively low inert gas pressure of  $\sim 8$  atm. For stoichiometric mixture at this pressure only 97% of conversion can be achieved (compare Fig. 1b and c).

Thus the thermodynamic calculation reveals that by conducting experiments under optimum gas pressure and adjusting the composition of the initial mixture one can expect the synthesis of product which involves only two solid phases SiC and MgO. The simple chemical treatment of such mixture (see details in [35]) allows complete leaching of the MgO phase and obtaining pure silicon carbide powder. However, the thermodynamics cannot suggest how one may control the microstructure of the product synthesized in the SHS wave. In this work the influence of the precursor's microstructure on the morphology and particles size of the produced SiC powder was investigated.

### 4. Experimental

Three different types of the silicon oxide ( $\text{SiO}_2$ ) powder were used: (i) from Yerken-deposit, Kazakhstan, (KZ) 98.8% purity, particle size  $d \leq 100$   $\mu\text{m}$ , (ii) Laboratory Cerac (LC), WI, USA,

Table 1  
Specific surface area (BET) of different  $\text{SiO}_2$  and SiC powders.

System/ powder	$\text{SiO}_2$	SiC as-leached		SiC as-leached
		BET ( $\text{m}^2/\text{g}$ )		Crystalline size (nm)
KZ	1	48	35	45
LC	7	71	54	40
UFS	390	104	83	24

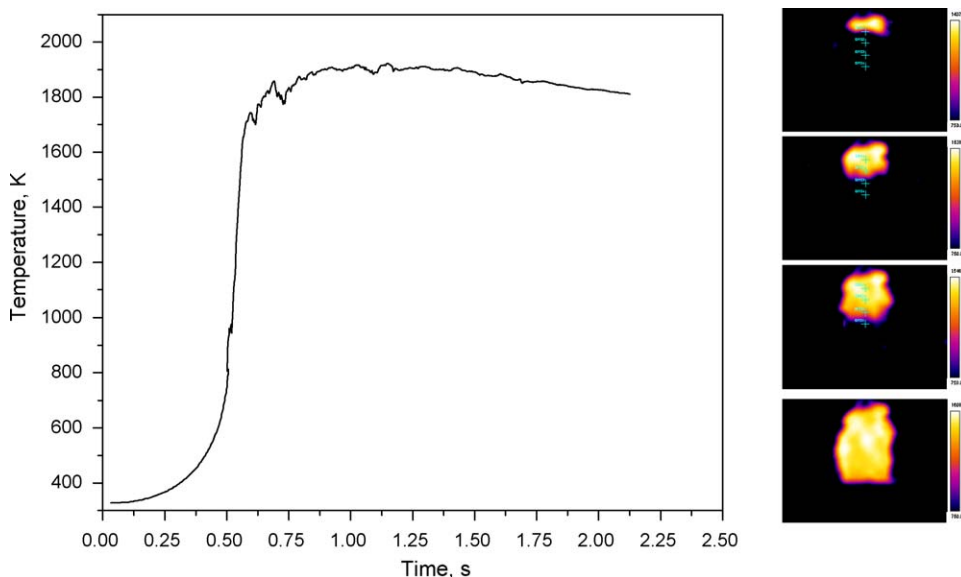


Fig. 3. IR video frames for the SHS process and typical temperature–time profile for combustion of  $\text{SiO}_2\text{--Mg--C}$  mixture ( $P = 1$  atm).

99.5% purity,  $d < 10 \mu\text{m}$  (iii) nano-Untreated Fumed Silica (UFS), Cabot Corporation, MA, USA, 99.9% purity. The typical microstructures of these powders are shown in Fig. 2 and Table 1 provides data on their specific surface area (BET). It can be seen that KZ powder has a wide range of particle size distribution with average size about  $20 \mu\text{m}$  and thus low specific surface area ( $1 \text{ m}^2/\text{g}$ ). Contrarily the UFS powder possesses extremely uniform and fine microstructure, as well as high BET  $\sim 390 \text{ m}^2/\text{g}$ . Laboratory Cerac (LC) powder has properties which are somewhere in between KZ- and UFS-silica with surface area  $\sim 7 \text{ m}^2/\text{g}$ . Carbon black powder and Mg (Alfa Aesar, MA, USA, 99.8% purity,  $d < 44 \text{ nm}$ ) were used as precursors for initial reactive mixture.

Correspondingly, three  $\text{SiO}_2\text{--Mg--C}$  mixtures (named below KZ, LC and UFC), using different silica, but with the same optimized compositions were prepared by 2 h of dry mixing. These mixtures were pressed using the automatic press-plant (Carver, Inc., USA) into cylindrical (diameter 1 cm; height 3 cm) samples with relative density TMD  $\sim 70\%$ , under the following conditions: maximum load 3000–5000 lbs, dwelling time 3 min, load rate 15%. All thus prepared samples were placed on graphite tray and inserted into a stainless steel cylindrical reactor with windows for the process diagnostic. The reactor was evacuated up to the  $10^{-3}$  atm and filled with argon up to the desired pressure, in the range of 1–20 atm. The ignition was carried out by a passing short electrical current impulse ( $I = 10 \text{ A}$ ,  $U = 20 \text{ V}$ ) through the coil of tungsten wire. Combustion temperature profile and average velocity of reaction front propagation were determined by using a high speed infrared camera (1FLIR Systems; model SC6000; Boston, MA).

All as-synthesized products were chemically treated for 3 h in 36% solution of hydrochloric acid at room temperature. The acid was taken into amounts according to the predicted mass of magnesium oxide to be leached out. This process was followed by thorough powder washing in ionized water and drying at  $100^\circ\text{C}$  for about 2 h.

The microstructure and phase composition of the powders were analyzed using XRD, SEM and BET methods. XRD analysis was carried out using Scintag Inc. X-ray diffractometer with  $\text{Cu K}\alpha$  radiation of wavelength  $1.54056 \text{ \AA}$ . Powder's morphology was analyzed by FEI field emission scanning electron microscopy (Magellan 400). The BET area measurements were made on a Quantachrome Corporation Autosorb-1 unit, which uses nitrogen as an adsorbent gas. Powders were

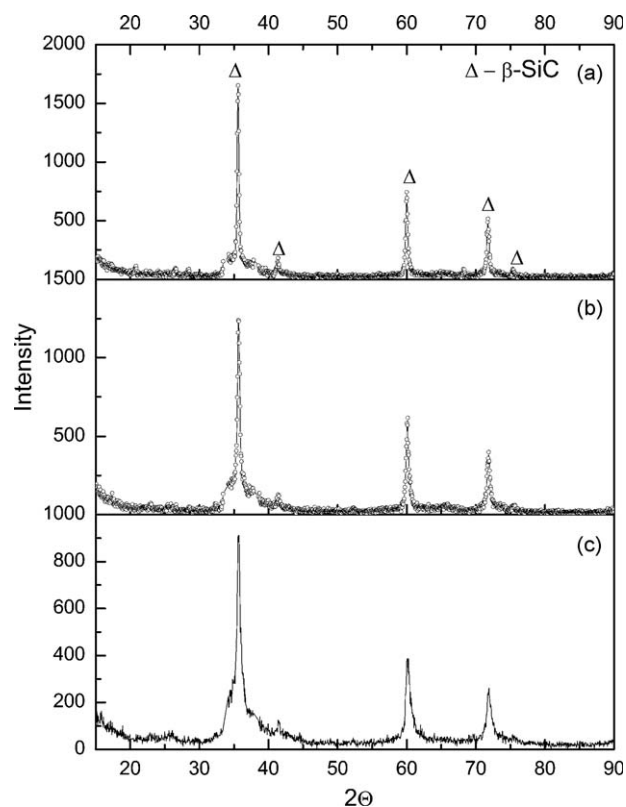


Fig. 4. Typical XRD-patterns for different SiC powders: (a) KZ; (b) LC; and (c) UFC.



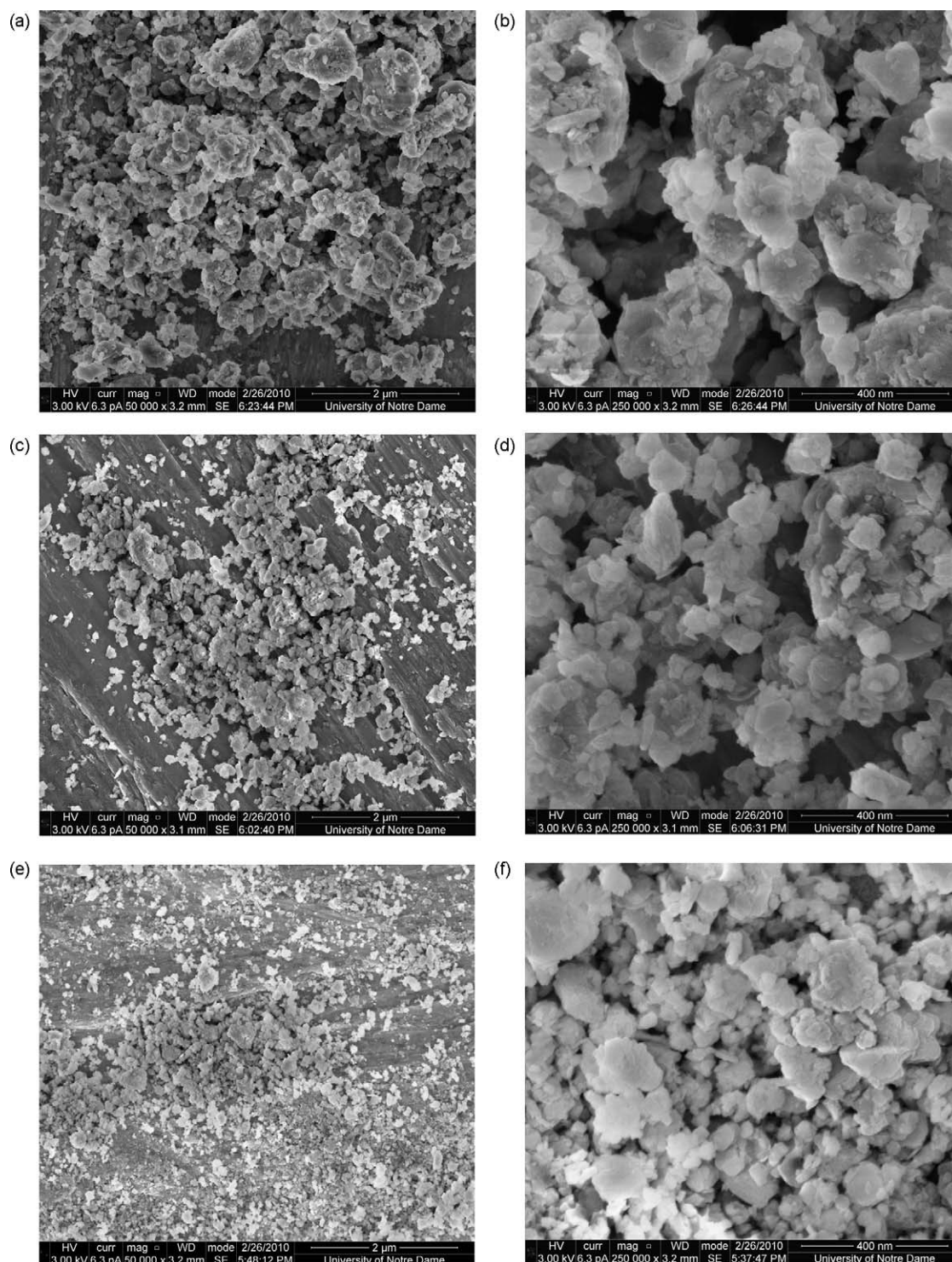


Fig. 5. Typical microstructure of different SiC powders: (a and b) KZ; (c and d) LC; (e and f) UFC.

outgassed at 473 K until the differential pressure falls below  $20 \mu\text{-Hg}$  per min. No other pretreatments were carried out prior to BET area measurements.

## 5. Results and discussion

Typical time–temperature profile for combustion front propagation in  $\text{SiO}_2\text{--Mg--C}$  system, for LC sample at

$P = 1 \text{ atm}$  obtained by IR-FLIR thermal vision apparatus is shown in Fig. 3. It can be seen that maximum combustion temperature ( $T_m = 1950 \text{ K}$ ) is only slightly below the calculated adiabatic temperature ( $T_{ad} = 2100 \text{ K}$ ). However, note that  $T_m$  is above the melting point of silica. It can be also seen that the combustion front is wide with duration of  $\sim 5 \text{ s}$ , which indicates the complexity of the reactions taking place during the SHS process. The analysis of IR-frames (one is shown in insert of

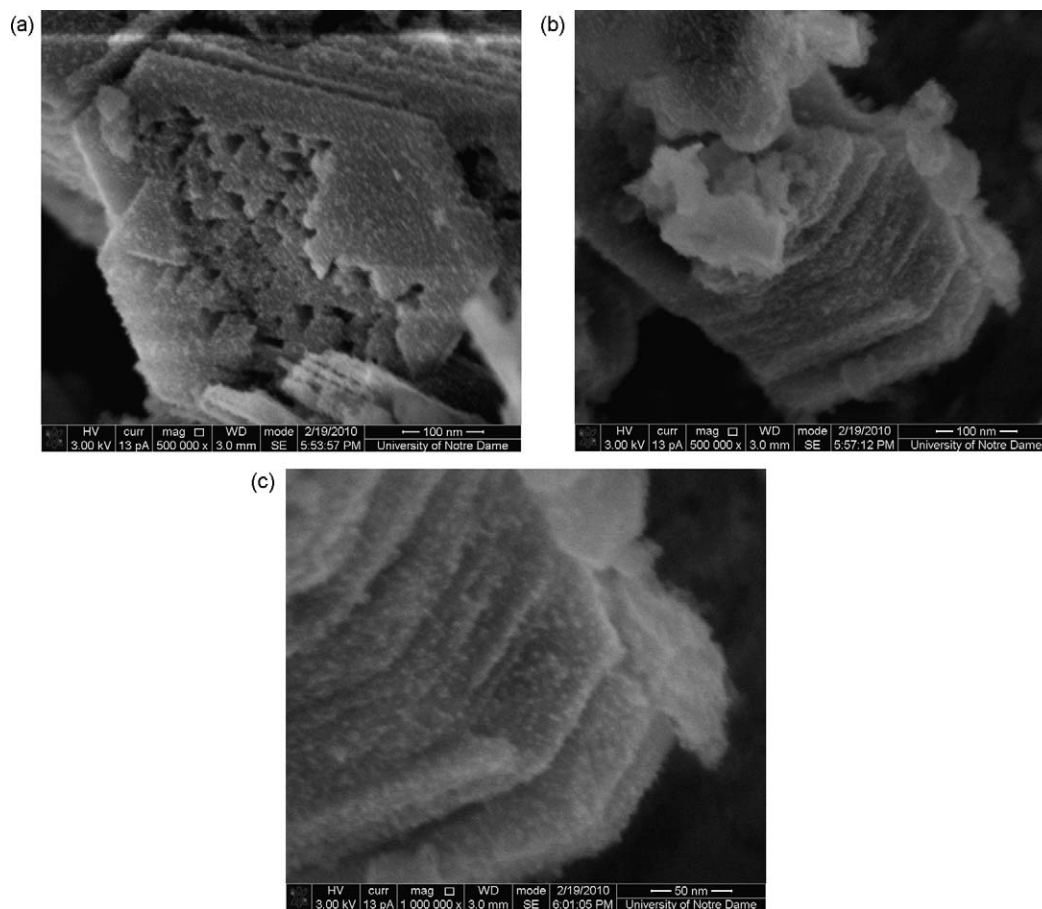


Fig. 6. Typical microstructure of SiC powder synthesized based on KZ-silica.

Fig. 3) shows that reaction front to propagate in steady state mode with average velocity  $v = 6.6 \pm 0.1$  cm/s. It is also important that  $T_m$  does not change for mixtures with different  $\text{SiO}_2$  powders, while the velocity of the combustion front increases with increasing silica surface area, from  $v = 3$  cm/s for KZ samples to  $v = 10$  cm/s for UFS. These observations can be explained based on the facts that: (i)  $T_m$  is close to  $T_{ad}$  and heat losses conditions were similar in all samples; (ii)  $\text{SiO}_2$  with higher surface allows more uniform infiltration of melted magnesium to silica skeleton, thus providing higher reactants contact area, which leads to higher rates of chemical reaction.

The set of XRD-patterns obtained for the leached silicon carbide powders synthesized from different silica is shown in Fig. 4. It can be seen that in all cases the only detected phase is  $\beta$ -SiC. However, further analysis of the XRD data shows that a significant decrease of SiC crystalline size occurred when one uses finer silica (see Table 1). These calculations were performed using the Scherrer equation:

$$\beta_{hkl} = \frac{K\lambda}{L_{hkl} \cos \theta_{hkl}}$$

where  $\beta$  is the width of the peak at half maximum intensity of a specific crystalline phase ( $h k l$ ) in radians,  $K$  is a constant equals to 0.95,  $\lambda$  is the wavelength of incident X-rays,  $\theta$  is the center angle of the peak in radians, and  $L$  is the length of the crystallite ( $\text{\AA}$ ). Data was taken from XRD scans obtained with

Cu  $K\alpha$  X-rays ( $\lambda = 1.54059 \text{ \AA}$ ), a  $0.02^\circ$  step size, and 0.5 s preset time. The peaks used for this analysis were  $2\theta = 59.291$  ( $1\ 1\ 0$ ) and  $71.965$  ( $1\ 1\ 15$ ).

The BET data confirm this conclusion showing (Table 1) a monotonic increase of powders specific area:  $48 \text{ m}^2/\text{g}$  for KZ-SiC;  $71 \text{ m}^2/\text{g}$  for LC-SiC and  $104 \text{ m}^2/\text{g}$  for USF-SiC. However, note that initial KZ-silica has about 400 times less  $\text{BET}_{ini}$  as compared to UFS-silica, while this large difference results only in two times higher  $\text{BET}_{ini}$  for the corresponding products. A logarithmic function  $\text{BET}_f = b \log(\text{BET}_{ini}) + a$ ; with  $a = 3.2$  and  $b = 21.2$  closely (Adj.  $R$ -square = 0.982) fits experimental data.

Microstructures of as-leached powders are shown in Fig. 5. It can be seen that all powders have relatively uniform particle size distribution with sub-micron average values:  $d_{KZ} = 280 \text{ nm}$ ;  $d_{LC} = 150 \text{ nm}$ ;  $d_{UFS} = 90 \text{ nm}$ . More close inspection (Figs. 6–8) reveals that in all cases particles involve a set of extremely thin hexagonal plates sintered to each other. The diagonal of the hexagon is about the average particle size, while thickness is as small as 10 nm for KZ-SiC (Fig. 6); 3–5 nm for LC-SiC (Fig. 7); and 1 nm UFS-SiC (Fig. 8).

Let us summarize the observed specifics of the microstructure transformations that take place in SHS wave of  $\text{SiO}_2$ –Mg–C systems. First, while two of the three precursors have micron size of heterogeneity, all silicon carbide powders are characterized by nanometer scale. Second, the smaller size of initial  $\text{SiO}_2$  powder leads to finer SiC particles with higher



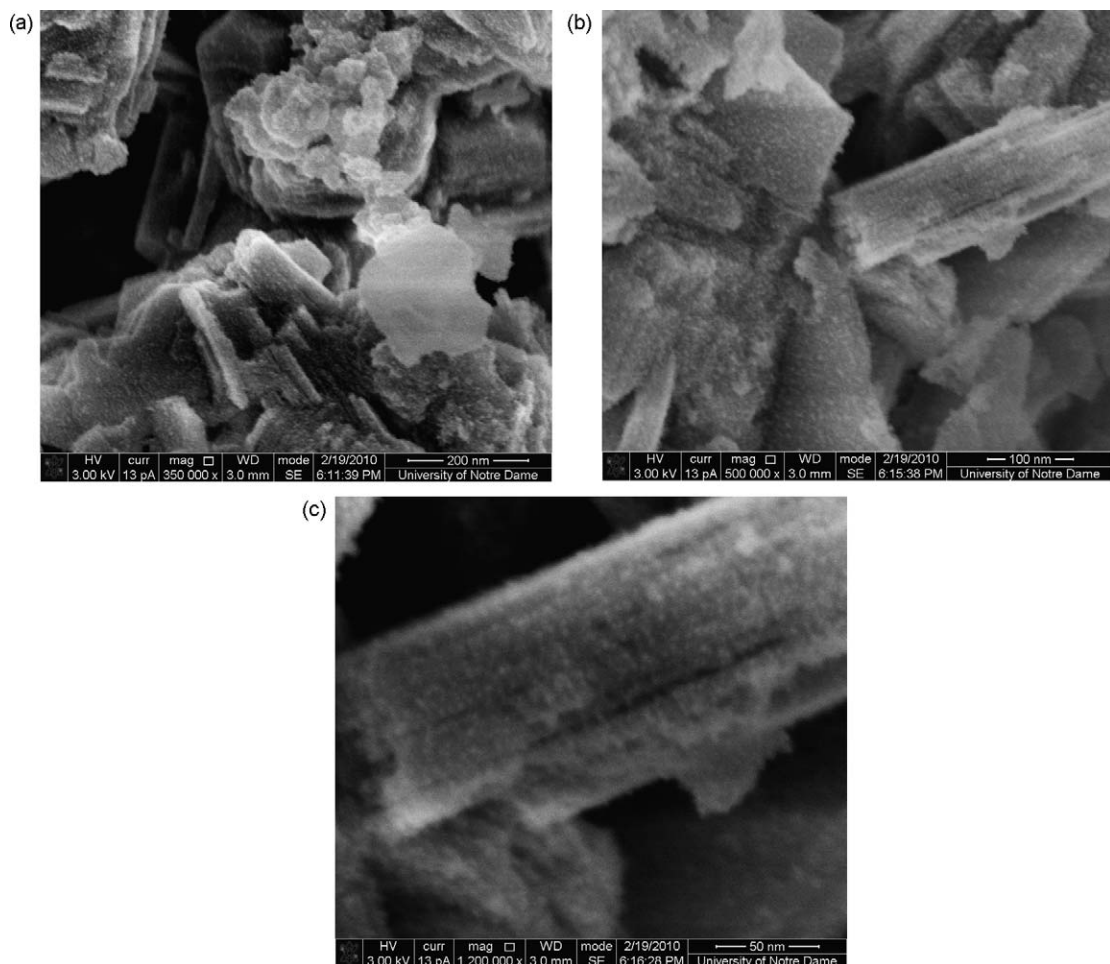


Fig. 7. Typical microstructure of SiC powder synthesized based on LC-silica.

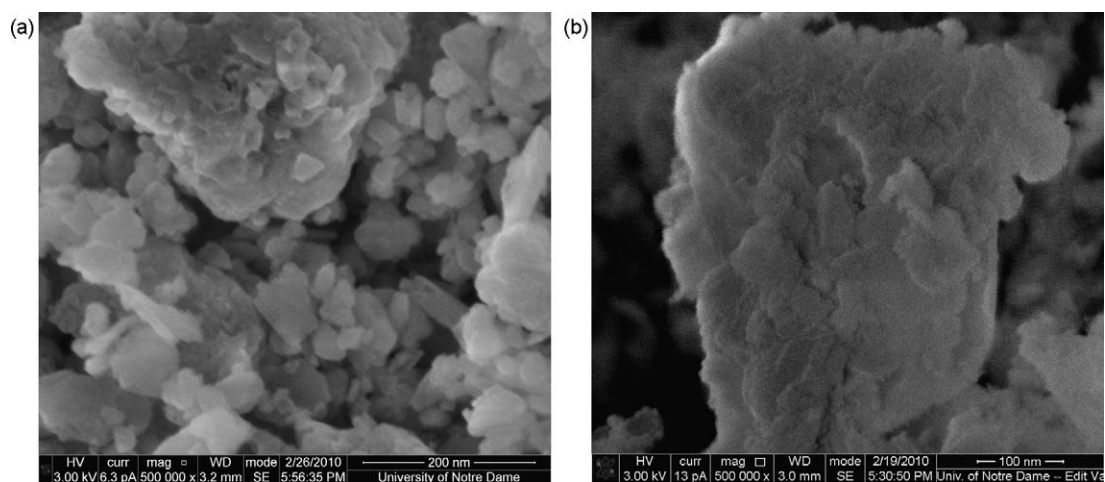


Fig. 8. Typical microstructure of SiC powder synthesized based on UFC-silica.

specific surface area. Third, for all precursors the morphology of the leached product involves sintered thin hexagonal-like plates of SiC grains. Also the maximum combustion temperature for all mixtures is above 2000 K and process duration is on the order of few seconds. Based on these results and taking into account our previous work in combustion

synthesis of pure silicon powders by reduction reaction in  $\text{SiO}_2 + \text{Mg}$  system [36], we may suggest the mechanism for silicon carbide formation in combustion wave.

As in the case of  $\text{SiO}_2\text{--Mg}$  system, at temperature 922 K magnesium melts and rapidly impregnates the silica skeleton with simultaneous reduction of oxide to silicon. The higher

surface area of SiO<sub>2</sub> skeleton provides higher contact area between Mg melt and SiO<sub>2</sub>, which leads to the reaction acceleration (compare velocities of the combustion front). Conducting experiments at high gas pressure (~8 atm) assures that evaporation (b.p. 1363 K at  $P = 1$  atm) of magnesium is eliminated, which is confirmed by full reduction of silicon oxide (see Fig. 4). When temperature reaches 1683 K, silicon melts and media structure involves the crystallization of solid MgO skeleton (~50 vol.%) with melted silicon matrix and fine solid carbon particles distributed in the melt. It is important that measured maximum combustion temperature in SiO<sub>2</sub> + 2Mg system [36] is also above 2000 K and only 200 K less than that for SiO<sub>2</sub> + 2Mg + C system, while the process durations is much shorter (1–2 s). Thus the reduction reaction producing silicon also brings the formed Si–C system to high temperature (>2000 K) at which the second, synthesis-type, reaction occurs. The microstructure of formed SiC particles suggests that this stage involves the dissolution of carbon in the silicon melt followed by its rapid crystallization. Because  $T_m$  is above the melting point of SiO<sub>2</sub> and SiC grains formed on the second stage of interaction owing to re-crystallization from the melt, their size does not have direct relation to the size of initial precursor. However, the size of SiC grains should correlate with the scale of heterogeneity of formed Si matrix, which, as it was shown previously [36], is on the order of 100–200 nm, and depends on the size of the initial oxide.

## 6. Conclusion

It is shown, that silicon carbon nanopowder can be directly synthesized by combustion reaction in the silica–magnesium–carbon system. While even micro-size precursors lead to formation of nano-particles, the scale of heterogeneity of used silica is a parameter which allows one to control the size of SiC grains. The  $\beta$ -SiC powder with surface area above 100 m<sup>2</sup>/g was synthesized.

## Acknowledgements

We gratefully acknowledge the Special Program for Education of the Graduate Students (*al-Farabi Kazakh National University, Kazakhstan*), which supported this research work. This work was also partially supported by Notre Dame Integrated Imaging Facility (NDIIF) and the Notre Dame Center for Environmental Science and Technology.

## References

- [1] W.J. Choyke, H. Matsunami, in: G. Pensl (Ed.), *Silicon Carbide: Recent Major Advances*, Springer-Verlag, Berlin, Heidelberg, New York, 2004.
- [2] T. Mizutani, K. Matsuhira, N. Yamamoto, *Advanced structural ceramics – from research to applications*, J. Ceram. Soc. Japan 114 (1335) (2006) 905–910.
- [3] Alan W. Weimer, in: William A. Weimer (Ed.), *Carbide, Nitride and Boride Materials: Synthesis and Processing*, Chapman & Hall, London, UK, 1997.
- [4] Jin-Seok Lee, Yun-Ki Byeun, Sang-Hoon Lee, Sung-Churl Choi, *In situ growth of SiC nanowires by carbothermal reduction using a mixture of low-purity SiO<sub>2</sub> and carbon*, J. Alloys Compd. 456 (2008) 257–263.
- [5] Shunlong Pan, Jingjie Zhang, Yanfeng Yang, Guangzhi Song, *Effect of process parameters on the production of nanocrystalline silicon carbide from water glass*, Ceram. Int. 34 (2008) 391–395.
- [6] H.-P. Martin, R. Ecke, E. Müller, *Synthesis of nanocrystalline silicon carbide powder by carbothermal reduction*, J. Eur. Ceram. Soc. 18 (1998) 1737–1742.
- [7] G.W. Meng, Z. Cui, L.D. Zhang, F. Phillipp, *Growth and characterization of nanostructured  $\beta$ -SiC via carbothermal reduction of SiO<sub>2</sub> xerogels containing carbon nanoparticles*, J. Cryst. Growth 209 (2000) 801–806.
- [8] Hongjie Wang, Yonglan Wang, Jihao Jin, *SiC powders prepared from fly ash*, J. Mater. Proc. Technol. 117 (2001) 52–55.
- [9] Wei Min Zhou, Bin Yang, Zhong Xue Yang, Feng Zhu, Li Jun Yan, Ya Fei Zhang, *Large-scale synthesis and characterization of SiC nanowires by high-frequency induction heating*, Appl. Surf. Sci. 252 (2006) 5143–5148.
- [10] P.J. Wellmann, R. Müller, D. Queren, S.A. Sakwe, M. Pons, *Vapor growth of SiC bulk crystals and its challenge of doping*, Surf. Coat. Technol. 201 (2006) 4026–4031.
- [11] Qian-Gang Fu, He-Jun Li, Xiao-Hong Shi, Ke-Zhi Li, Jian Wei, Zhi-Biao Hu, *Synthesis of silicon carbide nanowires by CVD without using a metallic catalyst*, Mater. Chem. Phys. 100 (2006) 108–111.
- [12] A. Ellison, B. Magnusson, B. Sundqvist, G. Pozina, J.P. Bergman, *SiC crystal growth by HTCVD*, Mater. Sci. Forum 457–460 (2004) 9–14.
- [13] A.G. Merzhanov, I.P. Borovinskaya, A.E. Sytchev, in: J.F. Baumard (Ed.), *Lessons in Nanotechnology from Traditional Materials to Advanced Composites*, SHS of Nano-powders, Techna Group Srl., Dijon, France, 2005.
- [14] A.G. Merzhanov, *The chemistry of self-propagating high-temperature synthesis*, J. Mater. Chem. 14 (12) (2004) 1779–1786.
- [15] S.T. Aruna, A.S. Mukasyan, *Combustion synthesis and nanomaterials*, Curr. Opin. Solid State Mater. Sci. 12 (2008) 44–50.
- [16] A.G. Merzhanov, I.P. Borovinskaya, A.E. Sytchev, in: J.F. Baumard (Ed.), *Lessons in Nanotechnology from Traditional Materials to Advanced Composites*, SHS of Nano-powders, Techna Group Srl., Dijon, France, 2005.
- [17] V.M. Martinenko, I.P. Borovinskaya, in: *Proceedings of the Third All-Union Conference on Technological Combustion*, Chernogolovka, (1978), p. 180.
- [18] J. Narayan, R. Raghunathan, R. Chowdhury, K. Jagannadham, *Mechanism of combustion synthesis of silicon carbide*, J. Appl. Phys. 75 (II) (1994) 7252–7257.
- [19] Osamu Yamada, Yoshinari Miyamoto, Mitsue Koizumi, *Self-propagating high-temperature synthesis of the SiC*, Mater. Res. Soc. 1 (1986) 275–279.
- [20] R. Pamdich, L. Stobierski, J. Lis, *Hot isostatically pressed alumina silicon carbide-whisker composites*, J. Am. Ceram. Soc. 72 (8) (1989) 1436–1438.
- [21] O. Yamada, K. Hirato, M. Koizumi, Y. Miyamoto, *Combustion synthesis of silicon carbide in nitrogen atmosphere*, J. Am. Ceram. Soc. 72 (9) (1989) 1735–1738.
- [22] Chien-Chun Wu, Chien-Chong Chen, *Direct combustion synthesis of SiC powders*, J. Mater. Sci. 34 (1999) 4357–4363.
- [23] H.H. Nersisyan, V.N. Nikogosov, S.L. Kharatyan, A.G. Merzhanov, *Chemical mechanisms of transformation and combustion regimes in silicon–carbon–fluoroplastic system*, Fiz. Gor. i Vzryva 6 (1991) 77–81.
- [24] S.L. Kharatyan, H.H. Nersisyan, *Combustion synthesis of silicon carbide under oxidative activation conditions*, Int. J. Self-Propagat. High-Temperature Synth. 3 (1) (1994) 17–25.
- [25] H. Chena, Y.G. Caoa, J.X. Tanga, S.Y. Tang, X. Chen, *Fabrication of large-scale SiC fibers using carbamide as additives*, J. Cryst. Growth 231 (2001) 4–7.
- [26] J. Zhang, J.C. Jeong, J.H. Lee, C.W. Won, D.J. Kim, C.O. Kim, *The effect of carbon sources and activative additive the formation of SiC powder in combustion reaction*, Mater. Res. Bull. 37 (2002) 319–329.
- [27] J.A. Puszynski, S. Miao, in: J.P. Singh (Ed.), *Innovative Processes/Synthesis: Ceramics, Glasses, Composites II. Chemically-assisted Combustion Synthesis of Silicon Carbide from Elemental Powders*, Am. Ceram. Soc., Westerville, 1998, pp. 13–21.
- [28] A. Feng, Z.A. Munir, *The effect of an electric field on self-sustaining combustion synthesis. Part II. Field assisted self-propagating synthesis of  $\beta$ -SiC*, J. Appl. Phys. 76 (3) (1994) 1927–1928.



- [29] Z.-G. Yang, L.L. Sbaew, Synthesis of nanocrystalline SiC at ambient temperature through high energy reaction milling, *Nanostruct. Mater.* 7 (8) (1996) 813–886.
- [30] Kun Yang, Yun Yang, Zhi-Ming Lin, Jiang-Tao Li, Ji-Sheng Du, Mechanical-activation-assisted combustion synthesis of SiC powders with polytetrafluoroethylene as promoter, *Mater. Res. Bull.* 42 (2007) 1625–1632.
- [31] A.G. Merzhanov, I.P. Borovinskaia, S.S. Mamian, G.V. Mikabidze, V.I. Vershinikov, G.F. Tavadze, Patent No. 4445557/26, C01B31/36, Russia (1994).
- [32] A.G. Merzhanov, I.P. Borovinskaia, N.S. Mahonin, L.S. Popov, Patent No. 4409571/26, C01B31/36, Russia (1992).
- [33] A.A. Shiryaev, Distinctive features of thermodynamic analysis in SHS investigations, *J. Eng. Phys. Thermophys.* 65 (1993) 957–962.
- [34] S.S. Mamyan, Thermodynamic analysis of SHS processes, progress in self-propagating high-temperature synthesis, *Book Ser.: Key Eng. Mater.* 217 (2002) 1–8.
- [35] A.P. Amosov, I.P. Borovinskaya and, A.G. Merzhanov, *Poroshkovaia tehnologia SVS materialov* (Powder Technology of SHS Materials), Mashinostroenie, Moscow, 2007.
- [36] Zh.S. Yermekova, Z.A. Mansurov, A.S. Mukasyan, Combustion synthesis of silicon nano powders, *Int. J. Self-Propagat. High-Temperature Synth.* 19 (2) (2010) 96–103.